FULL PAPER

Dalton
www.rsc.org/dalton

# A structural study of 1,8-bis(dimethyl phosphonito) naphthalene and related crowded chalcogeno derivatives

**Petr Kilian, Alexandra M. Z. Slawin and J. Derek Woollins***
*Department of Chemistry, University of St. Andrews, St. Andrews, Fife, UK KY16 9ST.*
*E-mail: jdw3@st-andrews.ac.uk*

***Received 27th August 2003, Accepted 2nd September 2003***
***First published as an Advance Article on the web 16th September 2003***

1,8-Bis(dimethylphosphonito) naphthalene Nap[P(OMe)$_2$]$_2$ (Nap = naphthalene-1,8-diyl) and a complete series of its mono- and di-oxidized phosphonato counterparts Nap[P(E)(OMe)$_2$]$_2$ (E = O, S, Se, lone pair and all their permutations) were prepared and fully characterized by X-ray crystallography and multinuclear NMR, IR, Raman and MS. Molecular distortion due to non-bonded substituent interactions was studied as a function of the bulk of the phosphorus substituents. The least and most strained molecules in the series are Nap[P(OMe)$_2$]$_2$ and Nap[P(Se)(OMe)$_2$]$_2$ with non-bonding P ··· P distances of 2.91 and 3.79 Å respectively.

## Introduction

The extent of steric strain in peri-substituted (1,8-disubstituted) naphthalenes is dictated by the interaction between peri-substituents, which can be repulsive, bridged or bonding. Obviously, the size of the peri-atoms as well as the number and size of atoms (groups) attached to them are also important. In peri-diphospha substituted naphthalenes with purely repulsive interactions between the peri-substituents, the steric strain is always significant.[1] Bridging of the peri-atoms *via* one or two bridging atoms (including proton or coordinated metal centre),[2] or formation of a direct peri-atom–peri-atom bond[3] leads to at least partial relaxation of the strain.

The availability of X-ray structural data plays a critical role in the assessment of the crowding. Various concepts are used to describe the strain; the P ··· P distance is the primary parameter in all of them. Further important parameters include the distances of the P atoms from the naphthalene mean plane (describing mainly the out-of-plane deformations and indicating the magnitude of concomitant organic backbone twisting), whilst the splay angle [P(1)–C(1)–C(10) + C(1)–C(10)–C(9) + C(10)–C(9)–P(9) − 360] reflects both in-plane and out-of-plane components of the strain. Thus, the magnitude of splay angle helps to distinguish between bonding (negative splay angle) and repulsion of peri-substituents (positive splay angle).[4]

Amongst the group of the most strained (repulsively interacting) 1,8-diphospha naphthalenes, all examples described in the literature possess tetrahedral or pseudo-tetrahedral (one position filled by a lone pair) coordinated P atoms. The size of a lone pair is less than that of non-hydrogen atoms, thus perhaps not surprisingly, less strain is observed in bis(phosphanyl) derivatives Nap(PR$_2$)$_2$ (Nap = naphthalene-1,8-diyl) than in bis(phosphanyl oxide) and chalcogenide derivatives Nap[P(E)R$_2$]$_2$ (E = O, S). Quite a large number of Nap(PR$_2$)$_2$ derivatives are known, on the other hand only a few structural studies of dioxidized Nap[P(E)R$_2$]$_2$ or intermediately oxidized Nap[P(E)R$_2$](PR$_2$) and [Nap(PR$_3$)(PR$_2$)]$^+$ have been reported (Fig. 1).[1b,c,5,6] The disulfurated derivatives Nap[P(S)Ph$_2$]$_2$ and particularly Nap[P(S)*t*BuPh]$_2$ showed significantly larger distortions than monoselenated, dioxide or phosphonium compounds.

In this comparative study we utilised the increased nucleophilicity of the phosphorus atom and the lesser bulk of the OMe groups in Nap[P(OMe)$_2$]$_2$ in order to accomplish diselenation and selenation–sulfuration. Unfortunately, we could not facilitate formation of the tellurium congener.

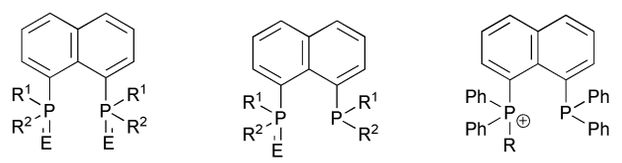


**Fig. 1** Previously structurally characterised, highly strained $\sigma^4,\sigma^4$ and $\sigma^4,\sigma^3$ 1,8-diphospha naphthalenes.[1b,c,5,6]

## Results and discussion

Compounds **1**–**10** were synthesized and their crystal structures were determined. Additionally, apart from the two previously reported compounds (**1** and **5**),[2c] all the new compounds were fully spectrally characterized by multinuclear NMR, IR, Raman and MS spectroscopy, the homogeneity of the new compounds was, where possible, confirmed by microanalysis.

### Syntheses of precursors 1 and 2

Two basic precursors **1** and **2** were used to access the remaining derivatives **3**–**10** (Schemes 1 and 2). Thus the methanolysis of Nap[P(NMe$_2$)$_2$]$_2$ afforded **1** in nearly quantitative yield (Scheme 1).

The methanolysis rate of Nap[P(NMe$_2$)$_2$]$_2$ was relatively slow, which facilitated $^{31}$P NMR detection of intermediates Nap[P(NMe$_2$)$_2$][P(OMe)(NMe$_2$)] (2 × d, $\delta_P$ 121.3 and 153.8 ppm, $^4J$(PP) = 246 Hz) and Nap[P(OMe)(NMe$_2$)]$_2$ (s, $\delta_P$ 121.1). We believe the assignment of $^{31}$P NMR signals to these species is fully justified due to the very distinct chemical shifts observed.[7]

Slow methanolysis of NapP$_2$Cl$_6$ at 0 °C in the presence of Et$_3$N resulted in a complicated mixture, containing disproportionation products Nap[P(OMe)$_2$]$_2$ (**1**) and Nap[P(O)(OMe)$_2$]$_2$ (**5**). Lowering of the reaction temperature to −40 °C improved the selectivity towards the desired monoxidized product **2** (Scheme 2), albeit *ca.* 10% of dioxidized compound **5** as well as small quantities of other by-products were still present in the mixture after reaction. Compound **2** was used for further syntheses as obtained, as the purification of the monoxidized products (**2**, **3** and **4**) proved to be rather difficult (*vide ultra*).

### Syntheses of monochalcogeno derivatives 3 and 4

The treatment of **1** with sulfur in 1 : 1 molar ratio led to a mixture of monoxidized product **3**, dioxidised product **6** and

DOI: 10.1039/b310392g

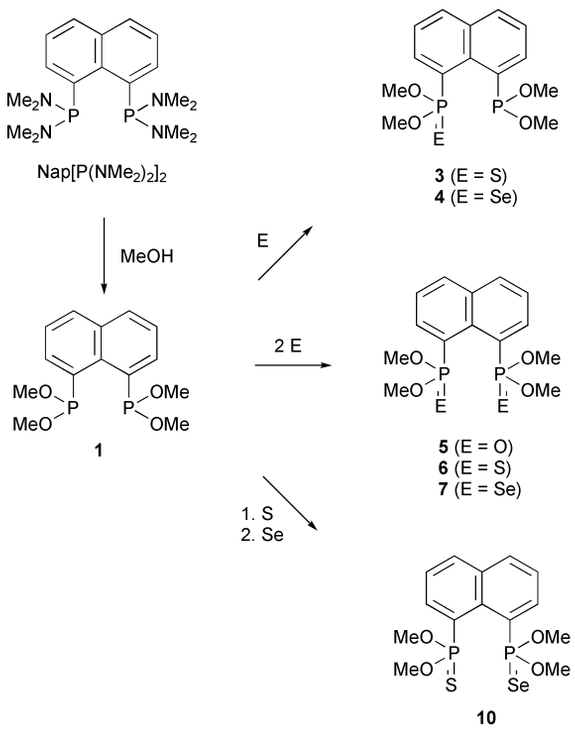


**Scheme 1** Syntheses from $Nap[P(NMe_2)_2]_2$.

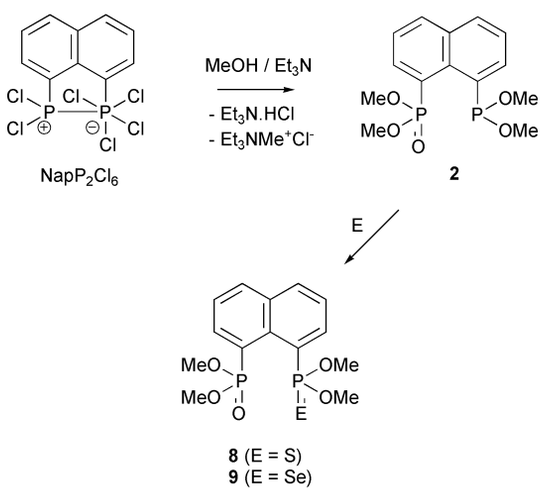


**Scheme 2** Syntheses from $NapP_2Cl_6$.

the starting bis(phosphonite). Variations of temperature as well as the slow addition of sulfur (in small batches) did not improve the selectivity towards the desired monooxidised product **3**. The starting material was easily removed by repeated recrystallization from hot hexane, but the removal of dioxidised product has proved to be significantly more difficult as its content remained constant (*ca*. 7%, assessed by $^1$H and $^{31}$P NMR) with repeated recrystallizations.

Essentially the same procedure as for the monosulfurated compound was used for the preparation of monoselenated congener **4**. Again, attempts to isolate pure **4** by repeated recrystallisation were not successful, and *ca*. 8% of dioxidized by-product **7** was present in the recrystallized material. However, due to the distinct habit of crystals **4** and **7**, it was possible to separate a small amount of pure **4** mechanically. Flash chromatography on silica was tested for the separation of monoxidized products **3** and **4** from their respective dioxidized by-products. Such a treatment, however, resulted in partial hydrolysis of both **3** and **4** towards phosphinic esters $Nap[P(E)(OMe)_2][P(H)(O)(OMe)]$ (E = S, Se).[8]

No reaction was observed on prolonged heating of $Nap(PPh_2)_2$ with elemental tellurium.[1c] Also prolonged heating of **1** with excess tellurium in toluene did not afford the desired telluride, even after the addition of a catalytic amount of base (DBU = 1,8-diazabicyclo[5.4.0]undec-7-ene).

### Syntheses of non-mixed dioxidized derivatives 5–7

Syntheses of **5**–**7** were straightforward and afforded high yields of pure products. Compound **5** had been prepared earlier by the action of the hydrogen peroxide/urea adduct on **1**.[2c] On attempts to repeat the procedure we observed contamination of the product **5** by substantial quantities of the phosphinic ester $Nap[P(O)(OMe)_2][P(H)(O)(OMe)]$, arising from hydrolytic side-reactions. Thus the alternative procedure using $O_2$ gas was employed, affording good yields of **5** free of hydrolytic product.

The reaction of **1** with sulfur was performed with external cooling due to its exothermic character. Using the standard selenation conditions (reflux with powdered grey selenium in toluene for few hours), a total conversion to the highly strained diseleno derivative **7** was achieved.

### Syntheses of mixed dioxidized derivatives 8–10

The reaction of **2** with one equivalent of S or Se, respectively, afforded O,S- and O,Se-mixed derivatives **8** and **9**. Flash chromatography on silica yielded pure compounds, albeit only in moderate yields.

For the synthesis of the S,Se-mixed congener **10**, the consecutive reaction of **1** with one equivalent of sulfur and then one equivalent of selenium was used. In this case flash chromatography was not employed in the purification of the product, as both by-products **6** and **7** as well as the desired **10** showed identical $R_f$ values in the TLC tests for various solvent systems; unfortunately, similar solubilities of all three compounds also prevented purification by repeated recrystallization.

It is clear, that the addition order of the chalcogens during the preparation of **10** can be swapped having little effect on the course of the reaction. Similarly, the oxidation of **3** and **4** with $O_2$ gas would afford the products **8** and **9**, respectively.

### NMR spectra

Selected NMR data of compounds **1**–**10** are summarized in Table 1. Unlike in the $Nap(PPh_2)_2$ congeners,[5] none of the $^1$H, $^{13}$C or $^{31}$P NMR spectra of **1**–**10** at 25 °C showed fluxional behavior due to hindered rotation about the P–C bonds. Even the most crowded molecules **6**, **7** and **10** show isochronous behavior of $^1$H and $^{13}$C nuclei in the series of chemically equivalent OMe groups, indicating that the arrangement of the phosphorus functionalities is not static or substantially hindered at 25 °C. We conclude that the lesser bulk of the OMe group compared to the Ph group results in a smoother motion of the OMe based molecular cogwheel.

The effect of the presence of the two proximate lone pairs confined in moderately crowded peri-space in **1** on the shielding of its $^{31}$P nuclei is not significant, *i.e*. only a slight shift to lower-frequency is observed in **1** ($\delta_P$ 151.7) compared to $PhP(OMe)_2$ ($\delta_P$ 159.0). More interestingly, the increased crowding in peri-space in mono- and di-oxidized derivatives **2**–**10** has no effect on their $^{31}$P shifts, as seen from comparison with non-crowded derivatives $PhP(O)(OMe)_2$ ($\delta_P$ 20.5), $PhP(S)(OMe)_2$ ($\delta_P$ 90.0) and $PhP(Se)(OMe)_2$ ($\delta_P$ 98.6).[9]

The $^4J$(PP) and $^5J$(PSe) couplings actually reflect the through-space P ··· P and P ··· Se interactions. Despite its fundamental importance, information on $^4J$(PP) coupling in 1,8-bis(phosphanyl) naphthalenes $Nap(PR_2)_2$ is very scarce, as its determination is complicated by several factors. There are no reports of unsymmetrical derivatives (with different chemical shifts of the two P atoms) allowing direct reading of $^4J$(PP) from $^{31}$P NMR spectra; the $^{13}$C satellite subspectra in $^{31}$P NMR does not allow its reading either as $^1J(P^{III}C)$ is relatively small and the satellites are hidden in the central line. The only

**Table 1** Selected NMR data of **1**–**10** (solutions in $CDCl_3$)

| Compound | **1** [a] | **2** | **3** | **4** | **5** [a] | **6** | **7** | **8** | **9** | **10** |
|---|---|---|---|---|---|---|---|---|---|---|
| Substitution pattern | –, – | O, – | S, – | Se, – | O, O | S, S | Se, Se | S, O | Se, O | Se, S |
| $\delta P^{III}$ | 151.7 | 161.0 | 159.1 | 159.3 | – | – | – | – | – | – |
| $\delta P^{V}$ | – | 24.0 | 90.4 | 96.6 | 20.7 | 89.3 | 94.7 | 20.9 and 89.9 | 20.0 and 95.2 | 89.7 and 95.3 |
| $^4J$(PP)/Hz | Not read [b] | 6.7 | 3.0 | 7.3 | <1 | 5.7 | 5.3 | 3.8 | 3.7 | 5.8 |
| $\delta C_{ipso}$ | 138.5 | 140.3 and 121.6 | 142.2 and 128.7 | 142.1 and 129.9 | 124.2 | 130.4 | 132.8 | 125.7 and 131.3 | 124.4 and 131.0 | 131.7 and 132.8 |
| $^1J$(CP)/Hz | 21.8 | 36.0 and 186.9 | 36.5 and 149.8 | 37.0 and 132.9 | 194.3 | 156.2 | 137.7 | 195.7 and 154.8 | 195.7 and 137.1 | 155.9 and 137.7 |

[a] Data taken from ref. 2*c*. [b] Nap[P(NMe$_2$)$_2$][P(OMe)(NMe$_2$)] showed $^4J$(PP) = 246 Hz, see text.

magnitude of 199 Hz reported to date was obtained from the MAS solid state $^{31}P\{^1H\}$ NMR spectrum of Nap(PPh$_2$)$_2$, the measurement was facilitated by inequivalence of the two P atoms in the molecule in the solid state.[10] Thus the magnitude of 246 Hz observed by us in the unsymmetrically substituted Nap[P(NMe$_2$)$_2$][P(OMe)(NMe$_2$)] intermediate (*vide infra*) is only the second reported to date; it is comparable with $^1J$(PP) in systems with a conventional $\sigma^3$P–$\sigma^3$P bond (the usual range being 180–230 Hz).

The monoxidized derivatives **2**–**4** also possess lone pairs available for through-space interaction. Interestingly, the magnitudes of through-space P ··· P interactions in the monooxidized derivatives Nap[P(E)(OMe)$_2$][P(OMe)$_2$] [E = O, S, Se, compounds **2**–**4**, $^4J$(PP) = 3.0–7.3 Hz, Table 1] were found to be much smaller than those in the two relatively similar systems Nap[P(E)Ph$_2$](PPh$_2$) [E = S and Se, $^4J$(PP) = 43 and 53 Hz][5] and Nap[P(S)Ph(*t*Bu)][PPh(*t*Bu)] [$^4J$(PP) = 40 and 42 Hz for the two diastereomeric forms **11** and **12**].[6] By way of contrast, the magnitudes of $^5J$(PSe) are very similar (and extraordinarily high) in both monoseleno derivatives Nap[P(Se)Ph$_2$](PPh$_2$) (54 Hz)[5] and Nap[P(Se)(OMe)$_2$][P(OMe)$_2$] (**4**, 61.1 Hz). As expected, the usual values of $^5J$(PSe) < 2 Hz were found in **7**, **9** and **10** as confirmed from both $^{31}$P and $^{77}$Se NMR spectra.

Based on the data above, we expect that molecules of Nap[P(E)Ph$_2$](PPh$_2$) (E = S, Se) and of Nap[P(S)Ph(*t*Bu)][PPh(*t*Bu)] in solution would populate a conformation in which the lone pair is positioned inside the peri-space and points towards the P$^V$ atom, whilst in **2**–**4**, the lone pair is rotated slightly off the peri-space, pointing not directly at the P$^V$ atom. In the same manner, the high magnitude of $^5J$(PSe) would indicate relative proximity of Se and P$^{III}$ atoms' lone pair in **4**. However, a comparison of crystal data of mixed valence P$^{III}$, P$^V$ systems with their solution NMR data did not give any simple correlations of $^4J$(PP) to P ··· P distance or to angular orientation of the P$^{III}$ atoms' lone pair with respect to the P$^V$ atom. Thus in the crystal of **4** a P ··· P distance identical to that in **11** (3.30 Å, Fig. 2) was found, yet contrasting magnitudes $^4J$(PP) 7 and 40 Hz were found in solution.[6] In the same manner, a nearly identical orientation of phosphorus' lone pair was found in the crystal of **4** and in Nap[P(Se)Ph$_2$](PPh$_2$) (n-P–C ··· P dihedral angles 8.8 and 7.2°, respectively, n = lone pair), yet the corresponding values of $^4J$(PP) were 7.3 and 53 Hz. This may reflect subtle differences between solid state and solution geometries.

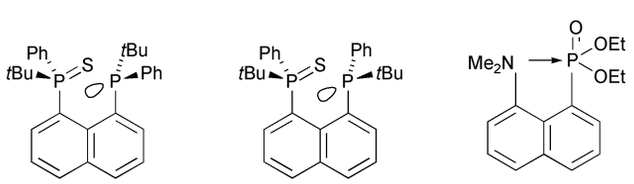


**11** **12** **13**

**Fig. 2** Two diastereomeric forms **11** and **12**; [4 + 1] coordinated phosphorus in **13**.

## Mass spectra

Apart from the usual fragmentation (loss of Me, OMe, *etc*.), the EI-MS spectra of **2**–**10** indicate cleavage of the P–C bond with loss of the –P(E)(OMe)$_2$ fragment (E = lone pair, S, Se). The preference of this pathway is very strong as the corresponding base (most abundant) peaks are formed. We believe that the release of steric strain is an important factor for the preference of this fragmentation mechanism.

## X-Ray investigations

The structures of compounds **1**–**10** in the crystal are shown in Fig. 3–5 and Tables 2 and 3. Compounds **1**–**5**, **8** and **9** crystallize with one molecule in the asymmetric unit, compounds **7** and **10** contain two nearly identical molecules in the asymmetric unit.

**Table 2** Selected bonding, non-bonding and displacement distances [Å], bond, torsion and dihedral angles [°] for **1**–**4**. For numbering of atoms see Fig. 3 and 4

| Compound | **1** | **2** [a] | **3** | **4** |
|---|---|---|---|---|
| Substitution pattern | –, – | –, O | –, S | –, Se |
| *Peri-region distances* | | | | |
| P(1)–C(1) | 1.846(4) | 1.795(2) | 1.810(5) | 1.809(3) |
| P(9)–C(9) | 1.834(4) | 1.832(2) | 1.855(5) | 1.842(3) |
| P(1)–E(1) | – | 1.465(2) | 1.937(2) | 2.0871(9) |
| P(1) ··· P(9); % of $\Sigma r_{vdW}$ [b] | 2.912(2); 77 | 3.238(4); 85 | 3.309(5); 87 | 3.299(2); 87 |
| P(9) ··· E(1); % of $\Sigma r_{vdW}$ [b] | – | 2.916(2); 85 | 3.281(4); 89 | 3.342(1); 88 |
| P(9) ··· O(11); % of $\Sigma r_{vdW}$ [b] | – | 3.382(7); 99 | 3.30(1), 96 | 3.249(4); 95 |
| *Out-of-plane displacement and dihedral angle* | | | | |
| P(1) | 0.31 | 0.77 | 0.76 | 0.73 |
| P(9) | 0.20 | 0.72 | 0.69 | 0.62 |
| P(1)–C(1) ··· C(9)–P(9) | 12.9 | 37.1 | 35.3 | 32.9 |
| *Peri-region bond angles* | | | | |
| Splay angle [c] | 9.6(3) | 11.3(2) | 14.6(4) | 15.3(3) |
| P(1)–C(1)–C(10) | 121.6(3) | 122.6(2) | 125.0(3) | 125.3(2) |
| P(9)–C(9)–C(10) | 122.0(3) | 123.0(2) | 122.2(4) | 123.5(2) |
| C(1)–C(10)–C(9) | 126.0(3) | 125.7(2) | 127.4(4) | 126.5(3) |
| *Central naphthalene ring torsion angles* | | | | |
| C(4)–C(5)–C(10)–C(1) | 4.4 | 10.4 | 10.3 | 9.1 |
| C(4)–C(5)–C(10)–C(9) | 177.6 | 169.7 | 169.3 | 170.2 |
| *Conformational angles* | | | | |
| E(1)=P(1)–C(1) ··· P(9) [d] | 36.8 | 53.6 | 61.4 | 62.8 |
| n-P(9)–C(9) ··· P(1) [e] | 36.1 | 18.5 | 10.2 | 8.8 |
| O(11)–P(1)–O(12) | 101.6(2) | 99.5(1) | 98.9(2) | 99.2(1) |
| O(13)–P(9)–O(14) | 101.4(2) | 100.8(1) | 101.0(2) | 101.7(1) |

[a] The terminal oxygen atom in the structure of **2** shows partial disorder. [b] The following van der Waals radii were used in the calculations: $r_{vdW}(P) = 1.90$, $r_{vdW}(O) = 1.52$, $r_{vdW}(S) = 1.80$, $r_{vdW}(Se) = 1.90$ Å. [c] Splay angle = P(1)–C(1)–C(10) + P(9)–C(9)–C(10) + C(1)–C(10)–C(9) − 360. [d] E = lone pair, O, S. Se; the position of the lone pair is calculated by reversing the direction of the vector from the phosphorus atom to the centre of gravity of its methoxy groups. [e] n = lone pair positioned on P(9), its position is calculated by reversing the direction of the vector from the phosphorus atom to the centre of gravity of its methoxy groups.

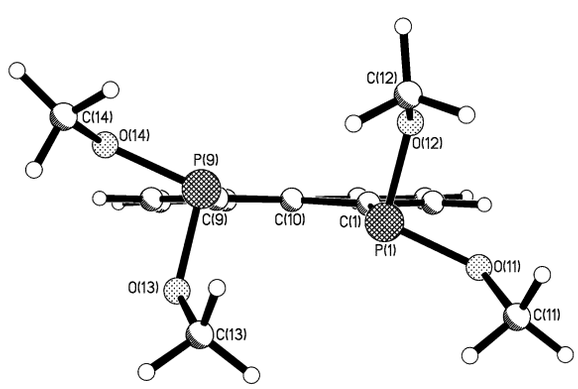


**Fig. 3** Structure of **1** in the crystal. The molecule is viewed along the central C(10)–C(5) bond to illustrate the extent of naphthalene ring twisting, out of plane displacements of phosphino groups and their mutual orientation.

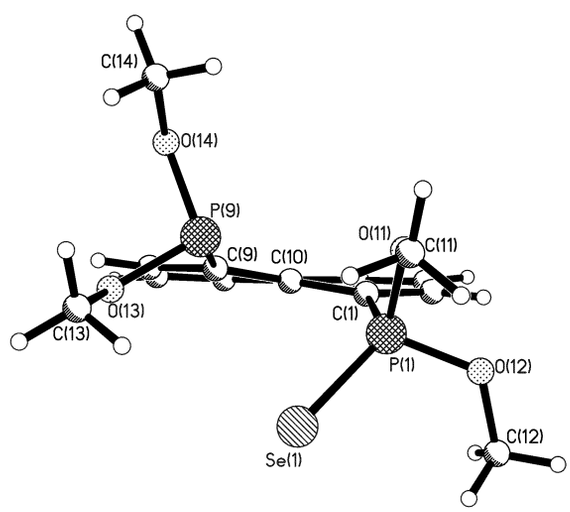


**Fig. 4** Structure of **4** in the crystal. The molecule is viewed along the central C(10)–C(5) bond to illustrate the extent of naphthalene ring twisting, out of plane displacements of phosphino groups and their mutual orientation.

A more symmetrical molecule ($C_2$) was found in the crystal of **6**, its asymmetric unit being half of the molecule. In all structures distinct twisting of the molecules is present and the phosphorus atoms are displaced to opposite faces of the best naphthalene plane. No short inter- or intra-molecular contacts between the chalcogen atoms were found in any of the compounds **1**–**10**.

The crystal structure of **1** is shown in Table 2 and Fig. 3. The molecule in the crystal has only approximate $C_2$ symmetry, the $C_2$ axis passing through atoms C(5) and C(10). The steric strain in molecule **1** is relatively low, as indicated by the relatively small displacement of its phosphorus atoms from the naphthalene best plane (0.31 and −0.20 Å) as well as relatively small, yet not negligible, splay angle (9.6°). The P ··· P non-bonding distance in **1** [2.912(2) Å] is only 77% of double the van der Waals radii, being the smallest in the series of compounds reported here. The P functionalities occupy a conformation in which the lone pairs are located inside the peri-space, although not pointing directly towards the other P atom. Essentially no other P ··· P sub-van der Waals contacts are present in the molecule. Previously, the conformations of P groups were "idealized" and described in relation to the naphthalene plane.[3a] However, in

**Table 3** Selected bonding, non-bonding and displacement distances [Å], bond, torsion and dihedral angles [°] for **5**–**10**. For numbering of atoms see Fig. 5 and 6

| Compound | **5** | **6** [a] | **7** [b] | **8** | **9** | **10** [b,c] |
|---|---|---|---|---|---|---|
| Substitution pattern | O, O | S, S | Se, Se | O, S | O, Se | S, Se |
| *Peri-region distances* | | | | | | |
| P(1)–C(1) | 1.809(2) | 1.812(2) | 1.812(3) [1.811(3)] | 1.816(3) | 1.802(6) | 1.812(5) [1.805(5)] |
| P(9)–C(9) | 1.806(2) | 1.812(2) [d] | 1.815(3) [1.816(3)] | 1.809(3) | 1.806(6) | 1.808(5) [1.809(4)] |
| P(1)–E(1) | 1.466(1) | 1.9334(7) | 2.0854(9) [2.0792(9)] | 1.930(1) | 2.074(2) | 2.022(1) [2.030(2)] |
| P(9)–E(9) | 1.465(1) | 1.9334(7) [d] | 2.0854(8) [2.0815(8)] | 1.462(2) | 1.467(4) | 2.044(2) [2.022(1)] |
| *Sub-van der Waals contacts in peri-region* [e] | | | | | | |
| P(1) ⋯ P(9); % of $\Sigma r_{vdW}$ [f] | 3.471(2); 91 | 3.737(2); 98 | 3.788(3); 100 [3.775(3); 99] | 3.595(1); 95 | 3.623(5); 95 | 3.773(4); 99 [3.756(4); 99] |
| Contact; % of $\Sigma r_{vdW}$ [f] | P(1) ⋯ O(9) 2.956(2); 86 | P(1) ⋯ O(12) 3.060(3); 89 | P(1) ⋯ O(14) 3.051(5); 89 [3.000(5); 88] | P(1) ⋯ O(9) 3.091(3); 90 | P(1) ⋯ O(9) 3.050(4); 89 | P(1) ⋯ O(13) 2.965(4); 87 [2.988(5); 87] |
| Contact; % of $\Sigma r_{vdW}$ [f] | P(9) ⋯ O(1) 3.024(3); 88 | P(9) ⋯ O(14) [d] 3.060(3); 89 | P(1) ⋯ O(12) 2.983(3); 87 [3.060(3); 89] | P(9) ⋯ O(11) 2.916(3); 85 | P(9) ⋯ O(12) 2.945(4); 86 | P(9) ⋯ O(11) 2.965(4); 87 [3.049(4); 89] |
| Contact; % of $\Sigma r_{vdW}$ [f] | O(9) ⋯ O(11) 2.833(3); 93 | | O(12) ⋯ O(14) 2.773(5); 91 [2.852(6); 94] | O(11) ⋯ O(13) 2.782(3); 91 | O(12) ⋯ O(9) 2.874(7); 94 | O(11) ⋯ O(13) 2.767(6); 91 [2.854(7); 94] |
| Contact; % of $\Sigma r_{vdW}$ [f] | O(1) ⋯ O(13) 2.871(2); 94 | | | | O(14) ⋯ O(12) 2.920(7); 96 | |
| *Out-of-plane displacement and dihedral angle* | | | | | | |
| P(1) | 0.78 | 0.90 | 0.94 [0.77] | 0.81 | 0.83 | 1.04 [0.77] |
| P(9) | 0.75 | 0.90 [d] | 1.04 [0.98] | 0.83 | 0.76 | 0.93 [0.98] |
| P(1)–C(1) ⋯ C(9)–P(9) | 39.1(1) | 44.7(1) | 50.9(2) [44.7(2)] | 40.9(2) | 39.8(4) | 50.9(3) [44.9(3)] |
| *Peri-region bond angles* | | | | | | |
| Splay angle [g] | 18.2 | 23.7 | 22.7 [25.3] | 21.1 | 23.0 | 21.9 [24.9] |
| P(1)–C(1)–C(10) | 126.5(1) | 127.7(2) | 128.5(2) [129.8(2)] | 128.8(2) | 129.6(4) | 126.7(4) [130.1(4)] |
| P(9)–C(9)–C(10) | 124.6(1) | 127.7(2) [d] | 126.9(2) [127.7(2)] | 124.6(2) | 125.6(4) | 128.8(4) [127.4(4)] |
| C(1)–C(10)–C(9) | 127.1(2) | 128.3(2) | 127.3(3) [127.8(3)] | 127.7(3) | 127.8(5) | 126.4(4) [127.4(4)] |
| *Central naphthalene ring torsion angles* | | | | | | |
| C(4)–C(5)–C(10)–C(1) | 8.9(3) | 11.6(1) | 11.8(4) [9.4(4)] | 10.0(5) | 12.1(8) | 10.8(7) [11.0(7)] |
| C(4)–C(5)–C(10)–C(9) | 170.0(2) | 168.4(2) | 167.9(3) [171.1(3)] | 167.9(3) | 167.6(5) | 169.1(4) [170.5(4)] |
| *Conformational angles* | | | | | | |
| E(1)–P(1)–C(1) ⋯ P(9) | 42.4(1) | 89.8(1) | 101.8(1) [94.7(1)] | 90.5(1) | 91.8(2) | 96.0(1) [94.6(1)] |
| E(9)–P(9)–C(9) ⋯ P(1) | 41.9(1) | 89.8(1) [d] | 95.9(1) [97.1(1)] | −41.7(1) | −36.7(2) | 102.2(1) [97.1(1)] |
| O(11)–P(1)–O(12) | 98.89(7) | 105.13(7) | 98.9(1) | 100.8(1) | 104.5(2) | 99.4(2) |
| O(13)–P(9)–O(14) | 99.18(8) | 105.13(7) [d] | 99.5(1) | 100.0(1) | 99.2(2) | 98.8(2) |

[a] Unit cell contains half of the molecule, crystallizes as **6**·$CH_2Cl_2$. [b] Values in square brackets are for the second independent molecule in the asymmetric unit. [c] The terminal S and Se atoms are disordered, the positions being in 50% of molecules occupied by S and in 50% by Se atoms. [d] By symmetry. [e] Only significantly sub-van der Waals contacts are listed. [f] The following values of van der Waals radii were used in calculations: $r_{vdW}$(P) = 1.90, $r_{vdW}$(O) = 1.52, $r_{vdW}$(S) = 1.80, $r_{vdW}$(Se) = 1.90 Å. [g] Splay angle = P(1)–C(1)–C(10) + P(9)–C(9)–C(10) + C(1)–C(10)–C(9) − 360.

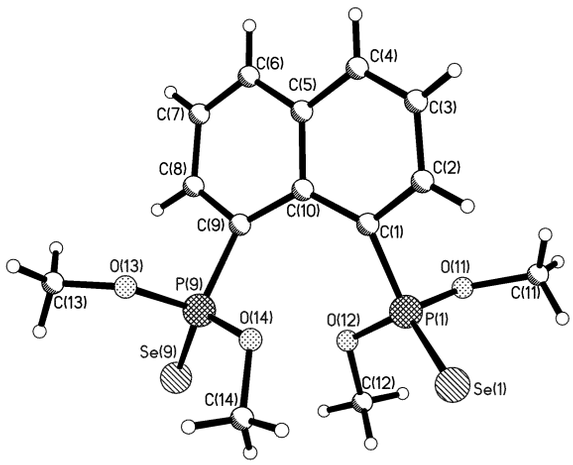


**Fig. 5** Structure of **7** in the crystal.

molecular cogwheels like **1**–**10**, the mutual relation of P functionalities is more important than their relation to the naphthalene moiety. Considering the relatively large and variable tilt of the C–P bonds from the naphthalene mean plane, we searched for a more convenient method of describing the conformation. Although not ideal, the dihedral angles E–P–C ··· P′ (E = O, S, Se or lone pair), listed in Tables 2 and 3, seem to be a more convenient way to describe the mutual positions of the two environments. Geometrically, the dihedral angles present the angle between the projection of P=E and P ··· P′ vectors along the P–C bond.

The structures of **2**–**4** in the crystal are shown in Table 2 and Fig. 4. The bond lengths and angles outside the peri-region are as usual. No approximate symmetry element can be found in the molecules of **2**–**4**, not surprising given their unsymmetrical substitution pattern. Despite this, the naphthalene skeleton is relatively symmetrical and the usual periodic alternation of C–C bond lengths takes place. The P–C distances are slightly shortened on oxidation from $P^{III}$ to $P^{V}$. Increased congestion of peri-space in **2**–**4** results in a larger displacement of P atoms from the naphthalene best plane (0.62–0.77 Å), the dihedral angle P(1)–C(1) ··· C(9)–P(9) being substantially increased to 32.9–37.0° compared to 12.9° in **1**. There is a relatively small change in the splay angle (maximum value 15.3° for **4** compared to 9.6° in **1**), whilst the deviation of the central naphthalene ring torsion angles from planarity is much more pronounced in the series of **2**–**4** (*ca*. 10° compared to *ca*. 4° in **1**). Quite surprisingly (given the difference in bulk of O, S and Se), all three monooxidized compounds occupy the same conformation. The terminal chalcogen atoms are turned slightly out of the peri-space compared to the lone pairs in **1**, whilst the $P^{III}$ lone pairs in **2**–**4** are oriented more inside the peri-space (towards the P ··· P abscissa) as illustrated by dihedral angles E(1)=P(1)–C(1) ··· P(9) 53.6–62.8° and n-P(9)–C(9) ··· P(1) 8.8–18.5°. The P functionalities interact mutually with sub-van der Waals P(1) ··· P(9) and P(9) ··· E(1) contacts, only just sub-van der Waals distances show P(9) ··· O(11) contacts. A similar conformation as in **2**–**5** was found in one of the two diastereomeric forms of **11**, the other form **12** showed a conformation with the main steric contacts through its phenyl ring rather than the sulfur atom.[6]

The structures of **5**–**10** in the crystal are shown in Table 3 and Fig. 5 and 6. Whilst the molecule **6** possesses a crystallographic $C_2$ axis, molecules **5** and **7** are less symmetric and possess only approximate $C_2$ axes. No symmetry element is present in asymmetrically substituted molecules **8**–**10**. Not surprisingly, the twisting in the dioxidized molecules **5**–**10** is substantially larger than that in the monoxidized series **2**–**4**, the P(1)–C(1) ··· C(9)–P(9) dihedral and splay angles range between 39 and 51° and 18.2 and 25.3°, respectively. The length of the P ··· P contacts in **5**–**10** reaching nearly 100% of the $\Sigma r_{vdW}$ shows that the main burden of steric strain is transferred to steric interactions with phosphorus substituents.

The importance of the length of the P ··· P contacts as an indicator of overall strain was discussed earlier. In diselenide **7** and sulfide–selenide **10** the P ··· P distances reach 3.76–3.78 Å, being comparable to those found in disulfides $Nap[P(S)Ph_2]_2$ [P ··· P distance 3.746(1) Å][1c] and $Nap[P(S)tBuPh]_2$ [P ··· P distance 3.832 Å – the longest known to date].[6] Parent phosphines of these disulfides – $Nap(PPh_2)_2$ and $Nap(PtBuPh)_2$ – represent the bulkiest diphosphino naphthalenes; attempts to prepare $Nap(PtBu_2)_2$ were not successful.[3a] The Ph and *t*Bu groups are obviously more bulky than the OMe groups, hence the diselenides $Nap[P(Se)Ph_2]_2$ and $Nap[P(Se)tBuPh]_2$ would presumably display even longer P ··· P distances. Unfortunately, the selenation of $Nap(PPh_2)_2$ under standard conditions gave only the monoselenide [displaying a P ··· P distance 3.248(1) Å].[5] We are not aware of any reports on selenation of $Nap[PtBuPh]_2$, however we presume that again only monoselenation may be accomplished as the energy gain connected with the formation of the second P=Se bond will probably be outweighed by increased strain in the diselenated product.

To overcome the problem of incomplete selenation, we used the less bulky OMe substituted derivative **1**, which rendered the diselenation possible. The overall strain in the resulting diselenide **7** is however equal to that found in the disulfides mentioned above, as the bigger bulk of the Se atom compared to the S atom is balanced by the lesser bulk of the methoxy groups. To conclude, we do not expect the existence of substantially more twisted diphospha naphthalenes with much longer P ··· P distances than *ca*. 3.8 Å.

The conformational variability in the group of dioxidized compounds **5**–**10** is interesting. Essentially three main conformers can be found among the group. In **5**, the terminal O atoms are oriented inside the peri-space, the bulk of the steric interaction being exerted by P(1) ··· O(9) and P(9) ··· O(1) sub-van der Waals contacts. In **6** (as well as in **7** and **10**), the

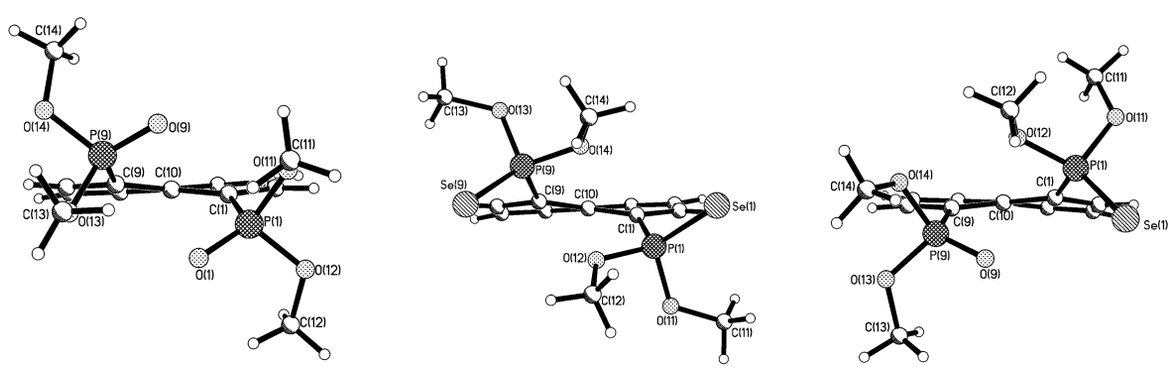


**Fig. 6** Structures of **5**, **7** and **9** in the crystal, the three conformation archetypes are shown. The molecules are viewed along the central C(10)–C(5) bond to illustrate the extent of naphthalene ring twisting, out of plane displacements of phosphino groups and their mutual orientation.

presence of larger sized S and Se atoms results in conformational flip-over. Methoxy groups now replace the terminal S and Se atoms in the peri-space, the sub-van der Waals contacts are observed mainly between the phosphorus atoms and oxygen atoms of the methoxy groups. The third conformation archetype, present in molecules **8** and **9**, is a half way between the two named conformations. The smaller terminal oxygen atom is located in the peri-space, whilst the larger S or Se atom is pointing out of it, which again leaves the oxygen atom of the methoxy group interacting at sub-van der Waals distances with atom P(9).

Despite the shortest P ··· O contacts in the series of compounds **5**–**10** being 2.916(3) Å (85% of $\Sigma r_{vdW}$), no distinct signs of rehybridization of tetrahedrally coordinated phosphorus atom into a trigonal bipyramidal (*TBPY*) configuration were observed. Related systems with forced N⟶P interactions have been intensely studied, *e.g.* in amino-phosphonate **13** N ··· P contacts accounting for 83% of $\Sigma r_{vdW}$ were found.[11] The authors claim that the phosphorus is [4 + 1] coordinated, however they describe the deformation of the P coordination environment as only slight.

## Conclusion

The reduced bulk of the parent diphosphonito naphthalene Nap[P(OMe)$_2$]$_2$ (**1**) rendered possible its diselenation to Nap[P(Se)(OMe)$_2$]$_2$ (**7**). The overall strain in **7** is found to be comparable to that in the most strained disulfide Nap[P(S)-*t*BuPh]$_2$, containing bulkier *t*Bu and Ph groups, but less bulky chalcogen.

The observed conformational variability in 1,8-diphospha naphthalenes is unprecedented, the size of the OMe groups (in contrast to Ph or *t*Bu) lying between the terminal O and S or Se allows for conformational control in the solid state. On the other hand, the series of monooxidized derivatives shows uniform conformations in the solid state.

## Experimental

All experiments were carried out in standard Schlenk glassware with the exclusion of air and moisture, only dioxidized products **5**–**10** can be handled in the air. Solvents were dried, purified, and stored according to common procedures.[12] Bis[bis-(dimethylamino)phosphano]naphthalene Nap[P(NMe$_2$)$_2$]$_2$ has been prepared from 1,8-dilithionaphthalene and chlorobis(dimethylamino)phosphane ClP(NMe$_2$)$_2$ as described in the literature,[13] phosphano-phosphorane NapP$_2$Cl$_6$ was prepared by chlorination of dithiadiphosphetane disulfide NapP$_2$S$_4$.[3c] All other reagents were obtained commercially. *In vacuo* refers to a pressure of ≈13 Pa. NMR: Bruker Avance 300 and JEOL GSX 270; 85% $H_3PO_4$ and $H_2SeO_3$ ($\delta_{Se}$ 1277 ppm) were used as external standards in $^{31}$P and $^{77}$Se NMR, $SiMe_4$ as internal standard in $^1$H and $^{13}$C NMR. All measurements were performed at 25 °C. Assignments of $^{13}$C and $^1$H NMR spectra were made with the help of $^1$H{$^{31}$P}, H–H COSY, H–C HMBC, H–C HSQC and H–P HMQC experiments (see Scheme 3 for atom numbering scheme). Raman (sealed capillaries) and IR (KBr tablets): Perkin-Elmer System 2000; MS: VG Autospec, electron energy 70 eV.

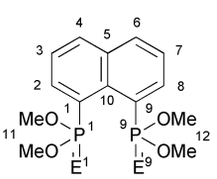


F.W. E1 > F.W. E9

**Scheme 3** Numbering scheme for NMR spectra of compounds **1**–**10**.

### Syntheses

**Nap[P(OMe)$_2$]$_2$ (1).** Nap[P(NMe$_2$)$_2$]$_2$ (5.5 g, 15.1 mmol) in THF (35 cm$^3$) and methanol (8 cm$^3$, 0.2 mol) were heated under reflux for 4 hours. The volatiles were evaporated *in vacuo* leaving red solid Nap[P(OMe)$_2$]$_2$. The purity of the product (assessed by $^{31}$P and $^1$H NMR) was sufficient for later syntheses; the content of color impurities can be substantially decreased by recrystallisation from hexane. Yield after recrystallization 4.14g (88%). A complete spectral characterisation of **1** was published previously.[3c] Some of the crystals obtained during recrystallization from hexane were suitable for X-ray work.

**Nap[P(O)(OMe)$_2$][P(OMe)$_2$] (2).** To an externally cooled (−40 °C) stirred suspension of NapP$_2$Cl$_6$ (3.00 g, 7.48 mmol) in 1,2-dimethoxyethane (50 cm$^3$) triethylamine (8 cm$^3$, 57.4 mmol) was added during 30 min; then methanol (2 cm$^3$, 49.4 mmol) was added during 1 hour. The resulting thick suspension was left to warm to ambient temperature and stirred for several hours. Precipitated $Et_3N{\cdot}HCl$ was filtered off, the filtrate was evaporated *in vacuo*, and THF (10 cm$^3$) was added, which led to precipitation of $Et_3NMe^+Cl^-$ in the form of a thick oil. The solution above this oil was separated and evaporated *in vacuo*. The resulting product **2** in the form of an oil was contaminated by dioxidised by-product Nap[P(O)(OMe)$_2$]$_2$ (*ca*. 10%, assessed by $^{31}$P NMR) as well as by other unidentified phosphorus-containing products (overall integral intensity *ca*. 8%). The oil partially solidified after standing for 1 day, removal of the remaining oil and washing of the solid with toluene (1 cm$^3$) and hexane (3 × 2 cm$^3$) gave a solid product, which was however only slightly less contaminated (1.10 g, 45%). Crystals suitable for X-ray work were obtained from an supersaturated toluene solution. IR: $\nu_{max}$/cm$^{-1}$ 2947m, 2926m, 2843m, 2824m (CH), 1459w, 1240s (P=O), 1050, 1023vs ((P)–O–C), 822, 776, 740, 720s (P–O–(C)), 592m; Raman: $\nu_{max}$/cm$^{-1}$ 3080 and 3048m (ArH), 2951, 2930m, 2846, 2827m (CH), 1558s, 1355s, 1341vs, 1152m, 895m, 597m, 525m, 457m, 321m; NMR ($CDCl_3$): $\delta_H$ (300 MHz) 3.58 [6H, d, $^3J$(HP) 12.8 Hz, H12], 3.69 [6H, d, $^3J$(HP) 11.3 Hz, H11], 7.37 [1H, ddd, $^3J$(HH) 8.2 and 7.2, $^4J$(HP) 2.8 Hz, H3], 7.48 [1H, m, $^3J$(HH) 7.9 and 7.3 Hz, H7], 7.79 [1H, m, $^3J$(HH) 8.1, $^4J$(HH) 1.4 Hz, H6], 7.89 [1H, m, $^3J$(HH) 8.2, $^4J$(HH) 1.4 Hz, H4], 8.01 [1H, ddd, $^3J$(HH) 7.2, $^4J$(HH) 1.5, $^3J$(HP) 10.0 Hz, H2], 8.22 [1H, ddd, $^3J$(HH) 7.3, $^4J$(HH) 1.3, $^3J$(HP) 3.8 Hz, H8]; $\delta_C$ (75.5 MHz) 51.8 [dd, $^2J$(CP) 6.6, $^6J$(CP) 4.4 Hz, C11], 53.8 [d, $^2J$(CP) 21.6 Hz, C12], 121.6 [dd, $^1J$(CP) 186.9, $^3J$(CP) 2.8 Hz, C1], 122.9 [d, $^3J$(CP) 16.0 Hz, C3], 125.0 [d, $^3J$(CP) 1.1 Hz, C7], 130.9 [d, $^4J$(CP) 2.2 Hz, C6], 131.1 [dd, $^2J$(CP) 5.0, $^4J$(CP) 1.1 Hz, C8], 132.5–133.2 (m, C10 and C5), 133.9 [m (second order), $^4J$(CP) 3.9 and 1.1 Hz, C4], 134.3 [d, $^2J$(CP) 7.2 Hz, C2], 140.3 [m (second order), $^1J$(CP) 36, $^3J$(CP) 3 Hz, C9]; $\delta_P$ (109.4 MHz) 24.0 (d, P1), 161.0 (d, P9), $^5J$(PP) 6.7 Hz; MS (CI+, ionizing gas isobutane): *m*/*z* 345 (C10H6[P(O)-(OMe)$_2$]$_2$ + H, oxidized product), 329 (M + H, base peak), 313 (MH − O), 297 (M − OMe), 283 ($C_{10}H_6PO(OMe)_2PHO$); accurate mass measurement on $^{12}C_{14}{}^1H_{19}{}^{16}O_5{}^{31}P_2$ (M + H) requires 329.0708, found 329.0708.

**Nap[P(S)(OMe)$_2$][P(OMe)$_2$] (3).** To a solution of **1** (0.400 g, 1.28 mmol) in toluene (10 cm$^3$) powdered sulfur (41 mg, 1.28 mmol) was added in small batches at 0 °C. The mixture was stirred for ½ hour at 0 °C and another 2 hours at ambient temperature. The resulting cloudy solution was filtered, the solvent was removed *in vacuo* and the remaining oil was vigorously stirred with hexane (10 cm$^3$) over night, which resulted in a thick suspension. The solid product was collected by means of filtration and recrystallized twice from hot hexane, giving a mixture of desired **3** (93%) with dioxidized product **6** (7%) (assessed by $^{31}$P and $^1$H NMR), 0.258 g (59%). Further recrystallizations did not affect the composition of the mixture. Crystals suitable for X-ray work were obtained from hot hexane/toluene. IR: $\nu_{max}$/cm$^{-1}$ 2942m, 2822m (CH), 1064s,

1048vs, 1023vs ((P)–O–C), 821vs, 780s, 770s, 735s, 716s (P–O–(C)), 648m, 498m; Raman: $\nu_{max}$/cm$^{-1}$ 3079, 3048m (ArH), 2944, 2825m (CH), 1554s, 1335vs, 890m, 560s, 310s; NMR ($CDCl_3$): $\delta_H$ (300 MHz) 3.55 [6H, dd, $^3J$(HP) 12.3, $^5J$(HP) <1 Hz, H12], 3.71 [6H, d, $^3J$(HP) 13.8 Hz, H11], 7.38 [1H, m (≈dt), $^4J$(HP) 2.7 Hz, H3], 7.51 [1H, m (≈t), H7], 7.81 [1H, m, $^3J$(HH) 8.2 Hz, H6], 7.88 [1H, dd, $^3J$(HH) 8.1, $^4J$(HH) 1.3 Hz, H4], 8.12 [1H, ddd, $^3J$(HH) 7.30, $^4J$(HH) 1.4, $^3J$(HP) 18.4 Hz, H2], 8.26 [1H, ddd, $^3J$(HH) 7.2, $^4J$(HH) 1.4, $^3J$(HP) 3.3 Hz, H8]; $\delta_C$ (75.5 MHz) 53.7 [dd, $^2J$(CP) 7.2, $^6J$(CP) 4.4 Hz, C11], 55.2 [d, $^2J$(CP) 21.0 Hz, C12], 124.2 [d, $^3J$(CP) 16.6 Hz, C3], 126.4 [d, $^3J$(CP) 1.1 Hz, C7], 128.7 [d, $^1J$(CP) 149.8 Hz, C1], 132.1 [dd, $^2J$(CP) 4.4, $^4J$(CP) 1.1 Hz, C8], 132.6 [d, $^4J$(CP) 2.2 Hz, C6], 133.0 [dd, $^3J$(CP) 27.1 and 12.7 Hz, C5], 134.2 [d, $^2J$(CP) 8.8 Hz, C2], 134.8 [dd, $^2J$(CP) 13.3 and 5.0 Hz, C10], 135.2 [dd, $^4J$(CP) 3.9 and ≈1.3 Hz, C4], 142.2 [dd, $^1J$(CP) 36.5, $^3J$(CP) 1.7 Hz, C9]; $\delta_P$ (109.4 MHz) 90.4 (d, P9) and 159.1 (d, P1), $^4J$(PP) 3.0; MS (EI+): *m*/*z* 344 ($M^+$), 329 (M − Me), 313 (M − OMe), 251[$C_{10}H_6PS(OMe)_2$, base peak], 189 ($C_{10}H_6P_2H$).

**Nap[P(Se)(OMe)$_2$][P(OMe)2] (4).** **1** (0.60 g, 1.9 mmol) and Se (0.167 g, 2.1 mmol) were heated under reflux in toluene (5 cm$^3$) for 2 hours, the resulting cloudy solution was filtered and checked by $^{31}$P NMR, which showed that it consisted of unreacted **1**, monooxidised product **4** (major component) and dioxidised product **7**. The oily residue remaining after the evaporation of solvent *in vacuo* was washed with hot hexane to remove **1** and the resulting solid was recrystallised from hot hexane/toluene to yield pale yellow crystalline **4** (0.175 g, 23%), contaminated by *ca*. 8% of **7**. Further recrystallizations did not affect the composition of the mixture. Crystals suitable for X-ray work were obtained from hot hexane/toluene. Due to the distinct habit of crystals of **4** and **7**, it was possible to separate a small amount of pure product **4** mechanically (mp 104–107 °C). Pure **4** was used for IR, Raman and MS; NMR spectra of **4** were measured as a mixture with *ca*. 8% of **7**. IR: $\nu_{max}$/cm$^{-1}$ 2939, 2821m (CH), 1332m, 1059vs, 1047vs, 1021vs and 1010vs ((P)–O–C), 811s, 769vs (P–O–(C)), 735s, 715vs, 597s, 529s; Raman: $\nu_{max}$/cm$^{-1}$ 3103m, 3079m, 3048m (ArH), 2941m, 2824m (CH), 1553vs, 1334vs, 888s, 531s, 472s, 303s; NMR ($CDCl_3$): $\delta_H$ (300 MHz) 3.56 [6H, dd, $^3J$(HP) 12.2, $^5J$(HP) < 1Hz, H12], 3.73 [6H, dd, $^3J$(HP) 14.5, $^5J$(HP) < 1 Hz, H11], 7.41 [1H, m (≈dt), $^4J$(HP) 2.6 Hz, H3], 7.52 [1H, dd (partially overlapped), H7], 7.84 [1H, m, $^3J$(HH) 8.1, $^4J$(HH) 1.3 Hz, H6], 7.88 [1H, m, $^3J$(HH) 8.2, $^4J$(HH) 1.1 Hz, H4], 8.13 [1H, ddd, $^3J$(HH) 7.30, $^4J$(HH) < 1, $^3J$(HP) 18.7 Hz, H2], 8.28 [1H, m, $^3J$(HH) 7.3, $^4J$(HH) 1.4 Hz, H8]; $\delta_C$ (75.5 MHz) 54.6 [dd, $^2J$(CP) 6.6, $^6J$(CP) 4.4 Hz, C11], 55.2 [d, $^2J$(CP) 20.4 Hz, C12], 124.2 [d, $^3J$(CP) 16.0 Hz, C3], 126.5 (s, C7), 129.9 [d, $^1J$(CP) 132.9 Hz, C1], 131.9 [dd, $^2J$(CP) 4.4, $^4J$(CP) 1.7 Hz, C8], 132.5 [d (partially overlapped), $^4J$(CP) 2.2 Hz, C6], 132.7 [dd (partially overlapped), $^3J$(CP) 27.1 and 12.7 Hz, C5], 133.8 [d, $^2J$(CP) 9.9 Hz, C2], 134.8 [dd, $^2J$(CP) 12.7 and 5.0 Hz, C10], 135.2 [dd, $^4J$(CP) 3.9 and 1.1 Hz, C4], 142.1 [dd, $^1J$(CP) 37.0, $^3J$(CP) 1.1 Hz, C9]; $\delta_P$ (109.4 MHz) 96.6 (d, P1) and 159.3 (d, P9), $^4J$(PP) 7.3 Hz, analysis of $^{77}$Se satellites yielded, $^1J$(PSe) 859, $^5J$(PSe) 61.1 Hz, analysis of $^{13}$C satellites of P1 confirmed $^1J$(P$^V$C) 132.9 Hz; $\delta_{77Se}$ (51.5 MHz) −209 [dd, $^1J$(PSe) 859, $^5J$(PSe) 61.1 Hz]; MS (EI+): *m*/*z* 392 ($M^+$), 377 (M − Me), 361 (M − OMe), 299 [$C_{10}H_6PSe(OMe)_2$, base peak], 189 ($C_{10}H_6P_2H$).

**Nap[P(O)(OMe)$_2$]$_2$ (5).** A solution of **1** (0.40 g, 1.28 mmol) in toluene (10 cm$^3$) placed in a 100 cm$^3$ round bottom flask was cooled to −80 °C and briefly evacuated. 50 cm$^3$ of oxygen gas was added using a syringe *via* a rubber septum, and the reaction mixture was heated to 70–80 °C for 24 hours. The solvent was evaporated *in vacuo* leaving a white solid, which was recrystallised from hot toluene/hexane to give pure **5** (0.356 g, 81%, assessed by $^{31}$P and $^1$H NMR). A complete spectral characterisation of **5** was published previously,[2c] we complement the spectroscopic characterization with Raman data. Some of the crystals obtained during recrystallization from toluene/hexane were suitable for X-ray work. Raman: $\nu_{max}$/cm$^{-1}$ 3072m and 3060m (ArH), 2951, 2849m (CH), 1561s, 1338vs, 910m, 766m, 597m, 325m.

**Nap[P(S)(OMe)$_2$]$_2$·CH$_2$Cl$_2$ (6·CH$_2$Cl$_2$).** To a solution of **1** (0.40 g, 1.28 mmol) in toluene (10 cm$^3$) powdered sulfur (84 mg, 2.62 mmol) was added at 0 °C. The mixture was stirred for 2 hours at ambient temperature, filtered, the solvent was removed *in vacuo*, and the remaining solid was recrystallised from dichloromethane/hexane to give pure **6** as a $CH_2Cl_2$ solvate (0.41 g, 69%), mp 144–145 °C. Crystals of **6**·$CH_2Cl_2$ suitable for X-ray work were obtained by slow evaporation of a $CH_2Cl_2$/hexane solution. Microanalysis was performed on a sample of crystalline **6**·$CH_2Cl_2$, which was partially desolvated (18 hours *in vacuo* at 20 °C) to $C_{14}H_{18}P_2O_4S_2$·0.4$CH_2Cl_2$: calcd. C 42.1, H 4.6; found C 42.1, H 4.6%. IR: $\nu_{max}$/cm$^{-1}$ 2982m, 2941m, 2834m (CH), 1491m, 1447m, 1026vs, 1004vs ((P)–O–C), 832, 821, 778s (P–O–(C)), 679m, 639m; Raman: $\nu_{max}$/cm$^{-1}$ 3075, 3054m (ArH), 2967m, 2945m, 2837m (CH), 1552s, 1330vs, 899s, 671s, 545s, 315s. NMR ($CDCl_3$): $\delta_H$ (300 MHz) 3.46 [12H, d, $^3J$(HP) 13.3 Hz, H11 and H12], 7.56 (2H, m, H3 and H7), 7.92 [2H, m, $^3J$(HH) 8.1, $^4J$(HH) 1.1 Hz, H4 and H6], 8.32 [2H, ddd, $^3J$(HH) 7.3, $^4J$(HH) 1.2, $^3J$(HP) 20.2 Hz, H2 and H8]; $\delta_C$ (75.5 MHz) 51.8 [m (second order), $^2J$(CP) 7.5, $^6J$(CP) <0.5 Hz, C11 and C12], 124.2 [m (second order), C3 and C7], 128.1 [t, $^2J$(CP) 5.8 Hz, C10], 130.4 [dd, $^1J$(CP) 156.2, $^3J$(CP) 2.5 Hz, C1 and C9], 132.3 [t, $^3J$(CP) 11.1 Hz, C5], 132.4 [m (second order), C4 and C6], 134.6 [m (second order), C2 and C8]; $\delta_P$ (109.4 MHz) 89.3(s), analysis of $^{13}$C satellites in $^{31}$P{$^1$H} spectrum yielded $^4J$(PP) 5.7 and confirmed $^1J$(PC) 156.2 Hz; MS (CI+, ionizing gas isobutane): *m*/*z* 433 (M + $C_4H_9$), 419 (M + $C_3H_7$), 377 ($MH^+$, base peak), 345 (M − S + H), 251 [$C_{10}H_6PS(OMe)_2$].

**Nap[P(Se)(OMe)$_2$]$_2$ (7).** **1** (0.40 g, 1.28 mmol) and Se (0.22 g, 2.79 mmol) were heated in toluene (5 cm$^3$) under reflux for 4 hours and the resulting suspension was hot filtered. The filtrate was concentrated to 2 cm$^3$ *in vacuo*. After standing overnight **7** precipitated in the form of pale yellow crystals, which were collected by filtration, washed with 2 × 0.5 cm$^3$ toluene and 2 cm$^3$ hexane and dried *in vacuo* (0.51 g, 84%), mp 154–156 °C (Found: C, 36.2; H, 3.5. $C_{14}H_{18}O_4P_2Se_2$ requires C, 35.8; H 3.9%). Some of the crystals were suitable for X-ray work. IR: $\nu_{max}$/cm$^{-1}$ 2986w, 2940m, 2835w (CH), 1587w, 1448m, 1175m, 1059vs, 1029vs and 1020vs ((P)–O–C), 817s, 767vs (P–O–(C)), 749s, 583s, 551s; Raman: $\nu_{max}$/cm$^{-1}$ 3063m, 3051m (ArH), 2943m, 2839w (CH), 1553vs, 1332vs, 895s, 535s, 311s; NMR ($CDCl_3$): $\delta_H$ (300 MHz) 3.44 [12H, d, $^3J$(HP) 13.8 Hz, H11 and H12], 7.56 (2H, m, H3 and H7), 7.93 [2H, m, $^3J$(HH) 8.2, $^4J$(HH) 1.1 Hz, H4 and H6], 8.35 [2H, ddd, $^3J$(HH) 7.3, $^4J$(HH) 1.3, $^3J$(HP) 21.0 Hz, H2 and H8]; $\delta_C$ (75.5 MHz) 54.2 [m (second order), $^2J$(CP) 7.6, $^6J$(CP) <0.5 Hz, C11 and C12], 125.6 [m (second order), C3 and C7], 128.2 [t, $^2J$(CP) 5.0 Hz, C10], 132.8 [dd, $^1J$(CP) 137.7, $^3J$(CP) ≈2.8 Hz, C1 and C9], 133.6 [t, $^3J$(CP) ≈10.2 Hz, C5], 134.0 [m (second order), C4 and C6], 136.3 [m (second order), C2 and C8]; $\delta_P$ (109.4 MHz) 94.7 (s with a set of $^{77}$Se satellites), analysis of $^{77}$Se and $^{13}$C satellite subspectra yielded $^4J$(PP) 5.3 and confirmed $^1J$(PSe) 891Hz, $^1J$(PC) 137.7; $\delta_{77Se}$ (51.5 MHz) −256 [d, $^1J$(PSe) 891 Hz]; MS (EI+): *m*/*z* 472 ($M^+$), 441 (M − OMe), 426 (M − OMe − O), 299 [$C_{10}H_6PSe(OMe)_2$, base peak].

**Nap[P(O)(OMe)$_2$][P(S)(OMe)$_2$] (8).** To a stirred solution of **2** (1.00 g, 3.05 mmol) in THF (7 cm$^3$) sulfur (98 mg, 3.05 mmol) was added and stirring was continued for 1 hour. The reaction mixture was filtered, the solvent was evaporated *in vacuo* to yield the crude product, which was purified using column chromatography on silica gel (eluent ethyl acetate) to yield a colorless, air stable solid **8** (0.351 g, 32%), mp 105–106 °C

(Found C 46.9, H 5.1. $C_{14}H_{18}O_5P_2S$ requires C 46.7, H 5.0%); IR: $\nu_{max}$/cm$^{-1}$ 2944m, 2839m (CH), 1493m, 1454m, 1265vs (PO), 1036vs ((P)–O–C), 832s, 813s, 776vs, 759vs (P–O–(C)), 632s; Raman: $\nu_{max}$/cm$^{-1}$ 3071m, 3039m (ArH), 2947m, 2841m (CH), 1555s, 1330vs, 902s, 556s; NMR ($CDCl_3$): $\delta_H$ (300 MHz) 3.534 [6H, d (partially overlapped), $^3J$(HP) 13.4 Hz, H11], 3.536 [6H, d (partially overlapped), $^3J$(HP) 11.1 Hz, H12], 7.54 (2H, m, H3 and H7), 7.93 (2H, m, H4 and H6), 8.12 [1H, ddd, $^3J$(HH) 7.2, $^4J$(HH) 1.4, $^3J$(HP) 17.3 Hz, H8], 8.35 [1H, ddd, 1H, $^3J$(HH) 7.3, $^4J$(HH) 1.4, $^3J$(HP) 19.6 Hz, H2]; $\delta_C$ (75.5 MHz) 52.9 [d, $^2J$(CP) 6.6, C12], 53.2 [d, $^2J$(CP) 7.7 Hz, C11], 125.1–125.7 (2 × d, C3 and C7), 125.7 [dd, $^1J$(CP) 195.7, $^3J$(CP) 2.2 Hz, C9], 131.3 [dd, $^1J$(CP) 154.8, $^3J$(CP) 3.3 Hz, C1], 131.5 [m (second order), C10], 133.7–134.3 [2 × dd overlapping with m (second order), C4, C6 and C5], 136.4 [dd, $^2J$(CP) 6.6, $^4J$(CP) <2 Hz, C8], 136.6 [dd, $^2J$(CP) 12.7, $^4J$(CP) <2 Hz, C2]; $\delta_P$ (109.4 MHz) 20.9 (d, P9) and 89.9 (d, P1), $^4J$(PP) 3.8 Hz; MS (EI+): *m*/*z* 360 ($M^+$), 329 (M − OMe), 313 (M − OMe − O), 251 [$C_{10}H_6PS(OMe)_2$, base peak], 189 ($C_{10}H_6P_2H$), 173 ($C_{10}H_6PO$). Crystals of **8** suitable for X-ray structure analysis were obtained by slow evaporation of the dichloromethane solution.

**Nap[P(O)(OMe)$_2$][P(Se)(OMe)$_2$] (9).** A mixture of **2** (0.50 g, 1.52 mmol) and powdered gray selenium (0.126 g, 1.60 mmol) was heated in toluene (10 cm$^3$) to 70 °C for 3 hours. The suspension was filtered and evaporated *in vacuo* to yield a yellow oil, which was purified using column chromatography (silica gel, eluent ethyl acetate) to yield a pale yellow air stable solid **9** (0.31 g, 50%), mp 96–99 °C (Found C 41.4, H 4.4. $C_{14}H_{18}O_5P_2Se$ requires C 41.3, H 4.4%); IR: $\nu_{max}$/cm$^{-1}$ 2951w, 2845w (CH), 1588m, 1567m, 1497m, 1384vs, 1278s (PO), 1041s and 917s ((P)–O–C), 765s (P–O–(C)), 602m; Raman: $\nu_{max}$/cm$^{-1}$ 3062m (ArH), 2951, 2847m (CH), 1558s, 1332vs, 901s, 558s, 535s, 318s; NMR ($CDCl_3$): $\delta_H$ (300 MHz) 3.514 [6H, d (partially overlapped), $^3J$(HP) 14.2 Hz, H11], 3.519 [6H, d (partially overlapped), $^3J$(HP) 11.0 Hz, H12], 7.53 (2H, m, H3 and H7), 7.93 (2H, m, H4 and H6), 8.10 [1H, ddd, $^3J$(HH) 7.3, $^4J$(HH) 1.3, $^3J$(HP) 17.1 Hz, H8], 8.39 [1H, ddd, $^3J$(HH) 7.3, $^4J$(HH) 1.3, $^3J$(HP) 20.6 Hz, H2]; $\delta_C$ (75.5 MHz) 51.6 [d, $^2J$(CP) 6.6 Hz, C12], 52.7 [d, $^2J$(CP) 7.7 Hz, C11], 124.0 [d, $^3J$(CP) 16.6 Hz, C3 or C7], 124.05 [d, $^3J$(CP) 18.2, C3 or C7], 124.4 [dd, $^1J$(CP) 195.7, $^3J$(CP) 2.2 Hz, C9], 129.5 [dd, $^3J$(CP) 10.0 and 5.5 Hz, C10], 131.0 [dd, $^1J$(CP) 137.1, $^3J$(CP) ≈3.6 Hz, C1], 132.5 [dd, $^2J$(CP) 11.1 and 12.7 Hz, C5], 132.9 [m (overlapped), C4 and C6], 135.0 [dd, $^2J$(CP) 6.6, $^4J$(CP) 1.1 Hz, C8], 135.6 [dd, $^2J$(CP) 15.5, $^4J$(CP) 1.7 Hz, C2]; $\delta_P$ (109.4 MHz) 20.0 (d, P9) and 95.2 [d with $^{77}$Se satellites, $^1J$(PSe) 889 Hz, P1], $^4J$(PP) 3.7 Hz; $\delta_{77Se}$ (51.5 MHz) −246 [d, $^1J$(SeP) 889 Hz]; MS (EI+): *m*/*z* 408 ($M^+$), 377 (M − OMe), 313 (M − O − Se + H), 299 ($C_{10}H_6PSe(OMe)_2$, base peak). Crystals of **9** suitable for X-ray structure analysis were obtained by precipitation from a highly supersaturated dichloromethane solution.

**Nap[P(S)(OMe)$_2$][P(Se)(OMe)$_2$] (10).** Powdered sulfur (51 mg, 1.60 mmol) was added to a solution of **1** (0.5 g, 1.60 mmol) in toluene (10 cm$^3$) at 0 °C. The mixture was stirred at 0 °C for ½ hour, left to warm to ambient temperature and stirred for an additional 2 hours before grey selenium (139 mg, 1.76 mmol) was added. The mixture was heated to 80 °C for 2 hours, filtered and the solvent was evaporated *in vacuo*. The crude product was recrystallised from hot toluene and toluene/hexane to yield 0.311 g (46%) of **10** contaminated by **6** (10%) and **7** (10%). Further recrystallizations did not affect the composition of the mixture. We were not successful in finding a suitable solvent system, which would allow separation of pure **10** by flash column chromatography, as the $R_f$ of the components were very similar. Crystals suitable for X-ray work were obtained from hot hexane/toluene. The following spectroscopic data were obtained using the contaminated product. IR: $\nu_{max}$/cm$^{-1}$ 2985m, 2942m, 2837m (CH), 1450m, 1061vs, 1024vs ((P)–O–

**Table 4** Crystallographic data for **1–10**

| Compound | **1** | **2** | **3** | **4** | **5** | **6** | **7** | **8** | **9** | **10** |
|---|---|---|---|---|---|---|---|---|---|---|
| Formula | $C_{14}H_{18}O_4P_2$ | $C_{14}H_{18}O_{5.15}P_2$ | $C_{14}H_{18}O_4P_2S$ | $C_{14}H_{18}O_4P_2Se$ | $C_{14}H_{18}O_6P_2$ | $C_{14}H_{18}O_4P_2S_2.CH_2Cl_2$ | $C_{14}H_{18}O_4P_2Se_2$ | $C_{14}H_{18}O_2P_2S$ | $C_{14}H_{18}O_5P_2Se$ | $C_{14}H_{18}O_4P_2SSe$ |
| Crystal habit | Colorless prism | Colorless prism | Colorless plate | Colorless plate | Colorless prism | Colorless prism | Colorless prism | Colorless prism | Colorless plate | Colorless prism |
| *M* | 312.22 | 330.62 | 344.28 | 391.18 | 344.22 | 461.27 | 470.14 | 360.28 | 407.18 | 423.24 |
| Crystal system | Orthorhombic | Monoclinic | Monoclinic | Monoclinic | Monoclinic | Monoclinic | Triclinic | Orthorhombic | Monoclinic | Triclinic |
| Space group | *Pna*2$_1$ | *P*2$_1$/*c* | *P*2$_1$/*c* | *P*2$_1$/*c* | *P*2$_1$/*n* | *P*2/*n* | *P*$\bar{1}$ | *P*2$_1$2$_1$2$_1$ | *P*2$_1$/*n* | *P*$\bar{1}$ |
| *a*/Å | 8.915(2) | 15.706(3) | 15.097(5) | 15.110(2) | 13.286(3) | 9.7707(19) | 9.962(1) | 8.712(1) | 9.115(2) | 9.889(1) |
| *b*/Å | 10.292(2) | 8.183(2) | 8.272(3) | 8.216(1) | 8.201(2) | 9.3104(18) | 14.375(2) | 11.376(1) | 16.300(4) | 14.326(2) |
| *c*/Å | 16.755(4) | 13.060(2) | 13.727(5) | 13.728(2) | 16.068(3) | 11.838(2) | 14.560(2) | 16.496(2) | 12.078(3) | 14.481(2) |
| *α*/° | 90.00 | 90.00 | 90.00 | 90.00 | 90.00 | 90.00 | 111.390(2) | 90.00 | 90.00 | 111.543(2) |
| *β*/° | 90.00 | 110.326(3) | 98.068(7) | 98.673(2) | 112.762(3) | 108.487(3) | 99.658(2) | 90.00 | 109.215(4) | 99.513(2) |
| *γ*/° | 90.00 | 90.00 | 90.00 | 90.00 | 90.00 | 90.00 | 108.660(2) | 90.00 | 90.00 | 108.494(2) |
| *U*/Å$^3$ | 1537.2(6) | 1574.0(5) | 1697.4(10) | 1684.7(4) | 1614.4(5) | 1021.3(3) | 1741.1(4) | 1634.9(4) | 1694.4(7) | 1714.8(3) |
| *Z* | 4 | 4 | 4 | 4 | 4 | 2 | 4 | 4 | 4 | 4 |
| *μ*/mm$^{-1}$ | 0.292 | 0.295 | 0.390 | 2.429 | 0.294 | 0.696 | 4.444 | 0.413 | 2.423 | 2.511 |
| No. of reflections: measured | 6058 | 8145 | 13312 | 6956 | 6593 | 4108 | 8680 | 5606 | 7215 | 8616 |
| independent | 1618 | 2228 | 2003 | 2386 | 2269 | 1418 | 4918 | 2895 | 2401 | 4834 |
| $R_{int}$ | 0.0596 | 0.0468 | 0.0397 | 0.0274 | 0.0227 | 0.0186 | 0.0462 | 0.0358 | 0.1411 | 0.0295 |
| $R$ ($F^2$, all data) | 0.0443 | 0.0538 | 0.0707 | 0.0354 | 0.0347 | 0.0296 | 0.0326 | 0.0528 | 0.0942 | 0.0646 |
| $wR$ ($F^2$, all data) | 0.0914 | 0.0871 | 0.1600 | 0.0747 | 0.0769 | 0.0715 | 0.0684 | 0.0819 | 0.1021 | 0.1298 |

C), 835s, 822s, 768vs (P–O–(C)), 633s, 562m; Raman: $\nu_{max}$/cm$^{-1}$ 3064m, 3052m (ArH), 2945m, 2840m (CH), 1554vs, 1333vs, 897s, 539s, 313m; NMR ($CDCl_3$): $\delta_H$ (300 MHz) 3.447 [6H, d (overlapped), $^3J$(HP) 13.3 Hz, H12], 3.450 [6H, d (overlapped), $^3J$(HP) 15.4 Hz, H11], 7.56 (2H, m, H3 and H7), 7.93 [2H, m, $^3J$(HH) ≈7.8 Hz, H4 and H6], 8.30 [1H, ddd (overlapped), $^3J$(HH) 7.3, $^4J$(HH) 1.3, $^3J$(HP) 19.8 Hz, H8], 8.36 [1H, ddd (overlapped), $^3J$(HH) 7.3, $^4J$(HH) 1.3, $^3J$(HP) 20.7 Hz, H2]; $\delta_C$ (75.5 MHz) 53.3 [d, $^2J$(CP) 7.7 Hz, C12], 54.1 [d, $^2J$(CP) 7.7 Hz, C11], 125.4–125.9 [2 × dd, C3 and C7], 128.9 [dd, $^2J$(CP) 6.1 and 4.4 Hz, C10], 131.7 [dd, $^1J$(CP) 155.9, $^3J$(CP) 2.8 Hz, C9], 132.8 [dd, $^1J$(CP) 137.7, $^3J$(CP) 2.8 Hz, C1], 133.7 [t, $^3J$(CP) 11.1 Hz, C5], 136.8–134.2 [2 × dd, C4 and C6], 136.0 [dd, $^3J$(CP) 13.3, $^5J$(CP) 1.7 Hz, C8], 136.3 [dd, $^3J$(CP) 15.5, $^5J$(CP) 1.1 Hz, C2]; $\delta_P$ (121.5 MHz) 89.7 (d, P1) and 95.3 [d with $^{77}$Se satellites, $^1J$(PSe) 891 Hz, P9], $^4J$(PP) 5.8 Hz; $\delta_{77Se}$ (51.5 MHz) −257 [d, $^1J$(PSe) 891 Hz]; MS (EI+): *m*/*z* 424 ($M^+$), 393 (M − S + H), 344 (M − Se + H), 299 [$C_{10}H_6PSe(OMe)_2$], 251 [$C_{10}H_6PS(OMe)_2$, base peak].

### Crystal structure analyses

All data were collected at 125 K on a Bruker SMART CCD diffractometer equipped with an Oxford Instruments low temperature attachment, using $Mo_{K\alpha}$ radiation ($\lambda$ = 0.71073 Å). Absorption corrections were performed on the basis of multiple equivalent reflections (SADABS[14]). All refinements were performed using SHELXTL.[14] See Table 4 for crystallographic data.

CCDC reference numbers 215965–215974.

See http://www.rsc.org/suppdata/dt/b3/b310392g/ for crystallographic data in CIF or other electronic format.

## References and notes


1 (*a*) A. Karacar, M. Freytag, P. G. Jones, R. Bartsch and R. Schmutzler, *Z. Anorg. Allg. Chem.*, 2002, **628**, 533–544; (*b*) A. Karacar, V. Klaukien, M. Freytag, H. Thonnessen, J. Omelanczuk, P. G. Jones, R. Bartsch and R. Schmutzler, *Z. Anorg. Allg. Chem.*, 2001, **627**, 2589–2603; (*c*) A. Karacar, M. Freytag, H. Thonnessen, J. Omelanczuk, P. G. Jones, R. Bartsch and R. Schmutzler, *Heteroatom Chem.*, 2001, **12**, 102–113.

2 See for example: (*a*) P. Kilian, A. M. Z. Slawin and J. D. Woollins, *Eur. J. Inorg. Chem.*, 1999, 2327–2333; (*b*) A. Karacar, H. Thonnessen, P. G. Jones, R. Bartsch and R. Schmutzler, *Chem. Ber./Recl.*, 1997, **130**, 1485–1489; (*c*) A. Karacar, M. Freytag, P. G. Jones, R. Bartsch and R. Schmutzler, *Z. Anorg. Allg. Chem.*, 2001, **627**, 1571–1581 and references therein.

3 (*a*) A. Karacar, M. Freytag, H. Thonnessen, P. G. Jones, R. Bartsch and R. Schmutzler, *J. Organomet. Chem.*, 2002, **643–644**, 68–80; (*b*) T. Mizuta, T. Nakazono and K. Miyoshi, *Angew. Chem., Int. Ed.*, 2002, **41**, 3897–3898; (*c*) P. Kilian, D. Philp, A. M. Z. Slawin and J. D. Woollins, *Eur. J. Inorg. Chem.*, 2003, 249–254.

4 For a discussion of various approaches see: G. P. Schiemenz, *Z. Anorg. Allg. Chem.*, 2002, **628**, 2597–2604.

5 A. Karacar, M. Freytag, H. Thonnessen, J. Omelanczuk, P. G. Jones, R. Bartsch and R. Schmutzler, *Z. Anorg. Allg. Chem.*, 2000, **626**, 2361–2372.

6 J. Omelanczuk, A. Karacar, M. Freytag, P. G. Jones, R. Bartsch, M. Mikolajczyk and R. Schmutzler, *Inorg. Chim. Acta*, 2003, **350**, 583–591.

7 Further data for comparison: $Nap[P(OMe)_2]_2$ ($\delta_P$ 151.7, ref. 2*c*), $Nap[P(NMe_2)_2]_2$ ($\delta_P$ 100.9, ref. 3*a*), $PhP(OMe)_2$ ($\delta_P$ 159.0, ref. 9), $PhP(NMe_2)_2$ ($\delta_P$ 100.3, ref. 9).

8 The rational syntheses and full characterization of the phosphinic esters will be published separately.

9 A. Schmidpeter and H. Brecht, *Z. Naturforsch., Teil B*, 1969, **24**, 179–192.

10 R. D. Jackson, S. James, A. G. Orpen and P. G. Pringle, *J. Organomet. Chem.*, 1993, **458**, C3–C4.

11 C. Chuit and C. Reye, *Eur. J. Inorg. Chem.*, 1998, 1847–1857.

12 D. D. Perrin and W. L. F. Armarego, *Purification of Laboratory Chemicals*, Pergamon Press, Oxford, 3rd edn., 1988.

13 A. Karacar, M. Freytag, H. Thonnessen, P. G. Jones, R. Bartsch and R. Schmutzler, *J. Organomet. Chem.*, 2002, **643–644**, 68–80.

14 G. M. Sheldrick, SADABS, Program for area detector adsorption correction, Institute for Inorganic Chemistry, University of Göttingen, Germany, 1996; G. M. Sheldrick, SHELXTL, version 5.10, Bruker AXS, Madison, WI, 1997.